The Plant Cell, Vol. 20: 2073–2087, August 2008, www.plantcell.org 

# The *milkweed pod1* Gene Encodes a KANADI Protein That Is Required for Abaxial/Adaxial Patterning in Maize Leaves [W]

**Héctor Candela,[a,b] Robyn Johnston,[c] Abigail Gerhold,[a,b] Toshi Foster,[c] and Sarah Hake[a,b,1]**

[a] Plant Gene Expression Center, U.S. Department of Agriculture–Agricultural Research Service, Albany, California 94710
[b] Plant and Microbial Biology Department, University of California, Berkeley, California 94720
[c] The Horticulture and Food Research Institute of New Zealand, Private Bag 11 030, Palmerston North, New Zealand

**Leaf primordia initiate from the shoot apical meristem with inherent polarity; the adaxial side faces the meristem, while the abaxial side faces away from the meristem. Adaxial/abaxial polarity is thought to be necessary for laminar growth of leaves, as mutants lacking either adaxial or abaxial cell types often develop radially symmetric lateral organs. The *milkweed pod1* (*mwp1*) mutant of maize (*Zea mays*) has adaxialized sectors in the sheath, the proximal part of the leaf. Ectopic leaf flaps develop where adaxial and abaxial cell types juxtapose. Ectopic expression of the *HD-ZIPIII* gene *rolled leaf1* (*rld1*) correlates with the adaxialized regions. Cloning of *mwp1* showed that it encodes a KANADI transcription factor. Double mutants of *mwp1-R* with a microRNA-resistant allele of *rld1*, *Rld1-N1990*, show a synergistic phenotype with polarity defects in sheath and blade and a failure to differentiate vascular and photosynthetic cell types in the adaxialized sectors. The sectored phenotype and timing of the defect suggest that *mwp1* is required late in leaf development to maintain abaxial cell fate. The phenotype of *mwp1; Rld1* double mutants shows that both genes are also required early in leaf development to delineate leaf margins as well as to initiate vascular and photosynthetic tissues.**

## INTRODUCTION

A fundamental question in developmental biology is how polarity is established and maintained during organogenesis. Plants are an attractive system to address this question because of the repetitive nature of leaf initiation. Leaves develop from a population of founder cells at the periphery of the meristem and exhibit polarity from the onset of initiation. The side of the leaf adjacent to the meristem, the adaxial side, has histological characteristics distinct from the abaxial side, the side furthest from the meristem (Kaplan, 1975; Steeves and Sussex, 1989). Proximal/distal polarity is also established upon leaf initiation, with the distal leaf tip growing away from the meristem. Finally, medial/lateral polarity is established at initiation by the presence of a midvein in the center of the leaf (Sharman, 1942; Esau, 1960). Although an inherent polarity exists in leaf primordia due to their relationship to the meristem, how polarity is maintained during leaf development as the leaf grows away from the meristem is not known.

A developmental genetic approach has provided insight into how abaxial/adaxial polarity is established and maintained in leaves. Phenotypic analyses in *phantastica* mutants of *Antirrhinum majus* provided the basis for an elegant model in which the juxtaposition of abaxial and adaxial cell fates leads to lamina growth (Waites and Hudson, 1995; Waites et al., 1998). Additional genes have been described that are specifically expressed in the abaxial or adaxial domains of the leaf (Kidner and Timmermans, 2007). *Arabidopsis thaliana kanadi1* (*kan1*) mutants were first identified in screens for the presence of trichomes in the abaxial epidermis of the first two rosette leaves, which normally lacks trichomes (Kerstetter et al., 2001), and as enhancers of mutations in *CRABS CLAW*, a *YABBY* gene that is required for abaxial identity in carpels (Eshed et al., 1999). Like the *YABBY* genes, *KAN1* and the other three *KAN* genes in *Arabidopsis* are expressed in lateral organs and encode transcription factors that redundantly specify abaxial fate. *kan1 kan2* and *kan1 kan2 kan3* loss-of-function mutants develop radial leaf primordia, abaxial outgrowths in the blade, and vascular bundles with xylem surrounding phloem (Eshed et al., 2001, 2004; Emery et al., 2003).

In contrast with the abaxial expression patterns of *KAN* genes, the transcripts of *HD-ZIPIII* genes are confined to the adaxial domain of lateral organs in wild-type plants (Zhong and Ye, 1999; Eshed et al., 2001; McConnell et al., 2001; Otsuga et al., 2001; Emery et al., 2003; Juarez et al., 2004b; Prigge et al., 2005; Williams et al., 2005). Several regulatory mechanisms contribute to this adaxial localization pattern. First, *HD-ZIPIII* transcripts are negatively regulated by two related microRNAs, miR165 and miR166 (Juarez et al., 2004b; Kidner and Martienssen, 2004; Williams et al., 2005). Mutations that disrupt the complementarity between *HD-ZIPIII* transcripts and these microRNAs behave as dominant, gain-of-function alleles that expand *HD-ZIPIII* expression outside of the adaxial domain (Zhong et al., 1999; McConnell et al., 2001; Emery et al., 2003; Zhong and Ye, 2004; Ochando et al., 2006). Such dominant mutations not only prevent transcript cleavage but have also been correlated with changes in the methylation levels of the corresponding chromosomal loci, suggesting that chromatin modifications also participate in the

[1] Address correspondence to maizesh@nature.berkeley.edu.
The author responsible for distribution of materials integral to the findings presented in this article in accordance with the policy described in the Instructions for Authors (www.plantcell.org) is: Sarah Hake (maizesh@nature.berkeley.edu).
[W] Online version contains Web-only data.
www.plantcell.org/cgi/doi/10.1105/tpc.108.059709

transcriptional silencing of *HD-ZIPIII* genes (Bao et al., 2004). Second, *KAN* genes function as genetic repressors of *HD-ZIPIII* transcripts, as inferred from the ectopic localization of *PHABULOSA* transcripts in *kan1 kan2 kan3* triple mutants and their downregulation by ectopic *KAN2* expression (Eshed et al., 2004). This antagonism between *KAN* and *HD-ZIPIII* genes provides a molecular mechanism for the generation of two discrete cell populations with mutually exclusive cell fates, as predicted by the juxtaposition model. Finally, the recent discovery of a family of small leucine zipper proteins, named LITTLE ZIPPER (ZPR), has added further complexity to the abaxial/adaxial patterning regulatory network (Wenkel et al., 2007; Kim et al., 2008). ZPR proteins are upregulated by HD-ZIPIII proteins and, in turn, negatively regulate HD-ZIPIII function by forming ZPR/HD-ZIPIII heterodimers that fail to bind DNA. Consistent with this model, overexpression of ZPR proteins yields an abaxialized leaf phenotype.

The maize (*Zea mays*) leaf has distinct proximal/distal and adaxial/abaxial domains, each with characteristic epidermal features and internal cellular organization (Sylvester et al., 1990). The proximal domain of the maize leaf is the sheath, which wraps around the culm and provides mechanical support to the leaf. The distal domain is the blade, which lays flat to optimize light capture and photosynthesis. The boundary between the sheath and blade is occupied by the ligule fringe and the auricles. The ligule extends across the leaf on the adaxial surface, sealing the space between the sheath and the stem to exclude potentially damaging external agents. The auricles, located on either side of the midrib, act as a hinge between sheath and blade. In maize, adaxial identity can easily be assessed by the presence of a ligule at the auricle-sheath boundary and by specific features, such as bulliform cells and macrohairs, in the blade domain. Combined with the large size of maize leaves, this rich diversity of anatomical and histological markers has facilitated the interpretation of mutant phenotypes resulting from local changes in polarity.

Maize leaf mutants that affect each of the three axes of polarity have been described. *Rolled leaf1* (*Rld1*) (Nelson et al., 2002; Juarez et al., 2004b), *leafbladeless1* (*lbl1*) (Timmermans et al., 1998; Juarez et al., 2004a; Nogueira et al., 2007), *ragged seedling2* (Henderson et al., 2005, 2006), *indeterminate gametophyte1* (*ig1*) (Evans, 2007), and *required to maintain repression6* (Parkinson et al., 2007) mutants affect abaxial/adaxial patterning in leaves. *Rld1* mutants are adaxialized and carry nucleotide substitutions at the miR166 complementarity site of the maize ortholog of the *HD-ZIPIII* gene *REVOLUTA* (Juarez et al., 2004b), indicating a regulatory interaction between *HD-ZIPIII* transcripts and miR166 that is conserved in *Arabidopsis* and maize. *lbl1* encodes a key component in the transacting small interfering RNA pathway, revealing that transacting small interfering RNAs are also important in leaf polarity (Nogueira et al., 2007). The *ig1* mutant, which identifies a role in abaxial/adaxial patterning for a LOB domain protein, illustrates the potential of maize for identifying subtle abaxial/adaxial polarity phenotypes (Evans, 2007).

Here, we describe the isolation and cloning of *milkweed pod1* (*mwp1*), a gene that is required for abaxial/adaxial patterning in the sheath domain. We show that *mwp1* encodes a member of the KAN family of GARP transcription factors. GARP is an acronym for the founding members in which the GARP DNA binding domain was originally found: maize Golden2, ARR B-class (*Arabidopsis* response regulators), and Psr1 (phosphorous stress response1 from *Chlamydomonas*) (Riechmann et al., 2000). The abaxial side is adaxialized in the sheath of *mwp1* leaves. The late onset of the phenotype, the sectored distribution of the phenotype, and the expression pattern in the epidermis are consistent with *mwp1* functioning in the maintenance of abaxial/adaxial polarity. Furthermore, adaxialized sectors in *mwp1* plants correlate with the ectopic expression of *rld1* mRNA. The synergistic phenotype of *mwp1; Rld1* double mutants shows that expression of *mwp1* and *rld1* is also needed early in development to pattern vasculature and photosynthetic tissues.

## RESULTS

### Recessive *mwp1* Mutations Alter the Abaxial/Adaxial Polarity of Sheath Tissues

The reference allele of *mwp1*, *mwp1-R*, is a spontaneous recessive mutation named after the resemblance of the husk leaf-enclosed ears to the seedpods of milkweed (*Asclepias syriaca*) plants. *mwp1-R* was introgressed into the W23, Mo17, A188, and B73 inbred backgrounds for more than three generations before characterizing the phenotype. Additional alleles were obtained by transposon tagging, as described below. The phenotype of *mwp1-R* is representative of the other alleles.

The *mwp1* phenotype is most pronounced on the outer, abaxial surface of husk leaves. Whereas wild-type husk leaves have smooth surfaces (Figures 1A and 1B), *mwp1-R* husk leaves are rough, with outgrowths that run longitudinally, in parallel to the proximal-distal axis (Figures 1H and 1I). To examine these outgrowths, we performed scanning electron microscopy and light microscopy analyses for both wild-type and mutant husk leaves. The adaxial epidermis of wild-type husk leaves is relatively smooth, with brick-shaped cells and short prickle-like hairs (Figure 1G). The abaxial epidermis has rounded cells and more hairs (Figure 1E) with especially long hairs near the margin (Figure 1F). Scanning electron microscopy revealed that the outgrowths on *mwp1-R* husk leaves occur in pairs (Figures 1J, 1K, and 1N). The outer surfaces of these flaps are hairy with rounded cells (Figure 1N), therefore resembling abaxial margin tissue. The inner surface of the ectopic flaps (Figure 1O) is smooth with brick-like cells and only short prickle-like hairs, similar to those in the adaxial epidermis (Figure 1G). In transverse sections, wild-type husk leaves have a slight ribbed appearance (Figure 1C) with widely spaced vascular bundles that have xylem at the adaxial pole and phloem at the abaxial pole (Figure 1D). In the ectopic flaps of *mwp1* husks, vascular bundles are oriented with xylem facing the adaxialized, inner side of the flaps (Figure 1K). Vascular bundles at junctions between flaps and the main lamina are often partially or fully radialized (Figure 1J, boxes), with xylem surrounding the phloem (Figures 1L and 1M). These phenotypes suggest that the ectopic flaps result from localized adaxialization of abaxial tissues and are consistent with the juxtaposition model (Waites and Hudson, 1995).

Given that the *mwp1* defect was first identified in husk leaves, which consist almost entirely of sheath tissue, we next examined

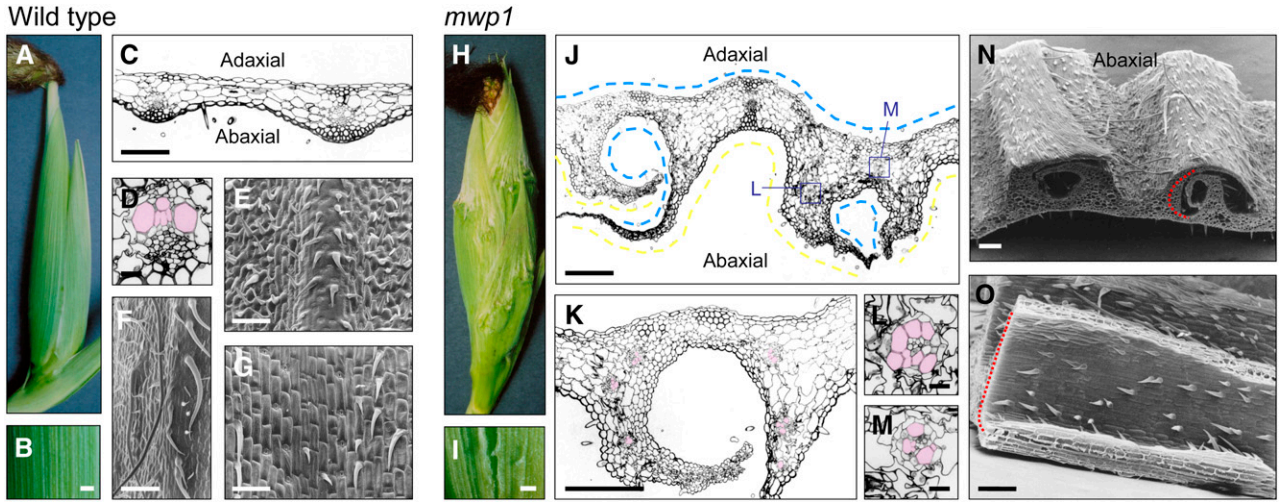


**Figure 1.** Phenotype of Wild-Type and *mwp1-R* Husk Leaves.

**(A)** to **(G)** Wild-type husk leaves.
**(A)** Wild-type ear covered by smooth husk leaves.
**(B)** Magnified view of the surface of a wild-type husk leaf.
**(C)** Transverse section through a wild-type husk leaf.
**(D)** Close-up view of a vascular bundle, showing a collateral distribution of adaxial xylem (pseudocolored pink) and abaxial phloem.
**(E)** Scanning electron micrograph of the abaxial epidermis.
**(F)** Scanning electron micrograph of the abaxial epidermis near the margin, showing characteristically long hairs.
**(G)** Scanning electron micrograph of the adaxial epidermis.
**(H)** to **(O)** *mwp1-R* husk leaves.
**(H)** *mwp1-R* ears are covered by rough husk leaves with outgrowths.
**(I)** Magnified view of the surface of a *mwp1-R* husk leaf.
**(J)** Transverse section through a *mwp1-R* husk leaf, showing the development of pairs of flaps flanking sectors of adaxialized epidermis on the abaxial side. Parts of the epidermis with adaxial and abaxial characteristics are indicated by blue and yellow lines, respectively.
**(K)** Magnified view of **(J)**, showing that the vascular bundles in the flaps have xylem oriented toward the inner, adaxialized side.
**(L)** and **(M)** Examples of radialized bundles from *mwp1-R* leaf flaps, with xylem at the periphery (pseudocolored pink).
**(N)** Scanning electron micrograph of a piece of *mwp1-R* husk leaf, showing the hairy outer surface of the flaps, characteristic of abaxial margin identity.
**(O)** Scanning electron micrograph of the inner surface of a flap, showing adaxial sheath characteristics.
Bars = 1 mm in **(B)** and **(I)**, 20 μm in **(D)**, **(L)**, and **(M)**, and 200 μm in all others.

the sheath of leaves on the main shoot for signs of adaxialization. Most *mwp1-R* leaves have an ectopic ligule on the abaxial surface at the auricle-sheath boundary (Figure 2F), at a location on the proximal/distal axis matching the normal, adaxial ligule (Figure 2A). Depending on the inbred background, the ectopic ligule may extend the entire width of the leaf or only a portion of the leaf (Figure 2F). Ectopic ligules were often associated with sectors of lighter green color in the sheath tissue immediately below. Transverse sections through normal sheaths revealed large vascular bundles alternating with intermediate bundles, both of which are connected to the epidermis through hypodermal sclerenchyma, and a few small bundles that are separated from the epidermis by several cell layers (Figure 2H) (Russell and Evert, 1985). Sections through the light-green sectors of *mwp1-R* sheaths revealed large, correctly patterned bundles alternating with groups of small bundles that are separated from the abaxial surface by proliferating ground tissue (Figure 2G). This defect may account for the lighter pigmentation and rough surface of the sectors. Because vascular patterning is a continuous, hierarchical process (Nelson and Langdale, 1992), this alternating pattern suggests that *mwp1* mutations do not disrupt the abaxial/adaxial polarity at the time of leaf initiation but rather that they fail to maintain organ polarity at a relatively late developmental stage.

Sectors of adaxialized sheath were also found at the base and margins of the sheath (Figures 2F and 2I), but no adaxialization defects were found in the blade (data not shown). The adaxialization at the base of the sheath tends to occur in bilaterally symmetric sectors that occasionally grow into irregularly shaped laminar projections (black arrow in Figure 2F). The adaxialization at the sheath margin, revealed by vertical patches of shiny, pale-green tissue on both sides of the sheath (Figure 2I), is accompanied by a blunt true margin and development of an ectopic flap on the abaxial side (Figure 2N). The margin of the ectopic flap was tapered, similar to normal sheath margins (Figure 2L). The epidermis between the true and ectopic margins was smooth and similar to normal adaxial epidermis, whereas the rest of the abaxial epidermis was hairy (Figure 2I). The vascular bundles near the true margin of *mwp1-R* leaves had xylem on both poles and phloem at the center (Figures 2O and 2Q), in contrast with

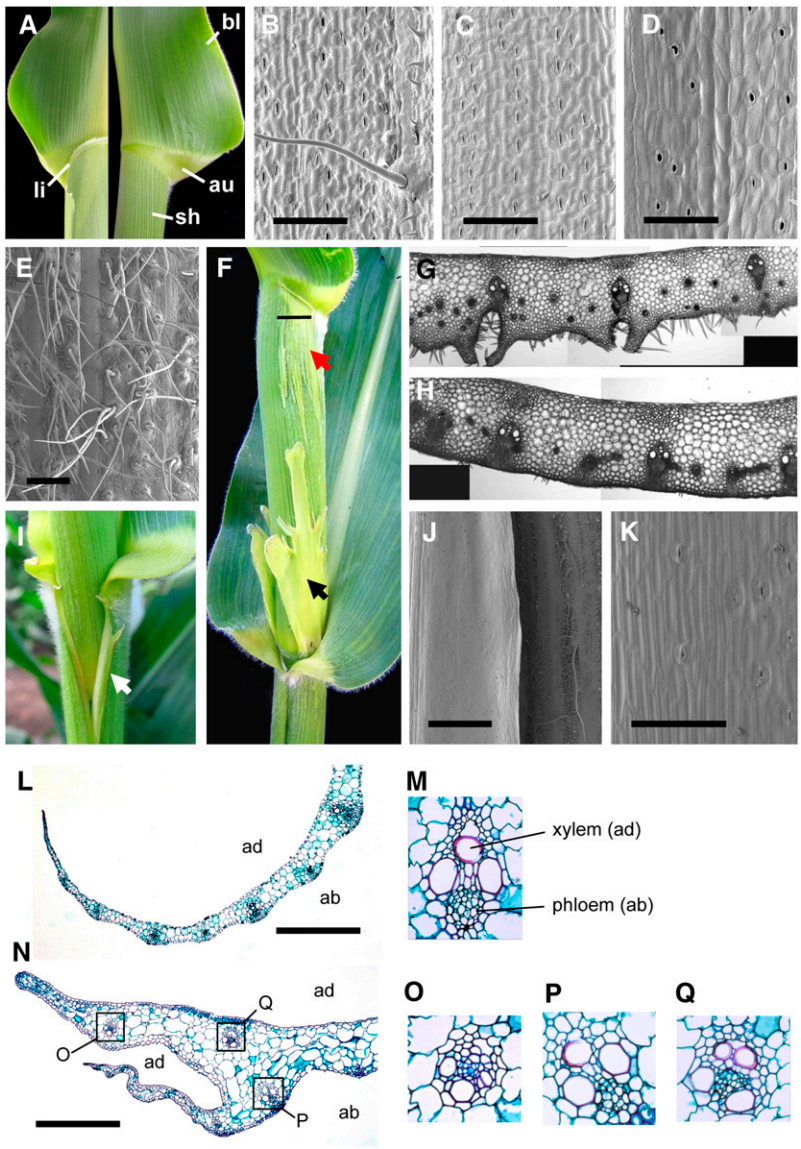


**Figure 2.** The *mwp1* Phenotype in Vegetative Leaves.

**(A)** Wild-type leaves consist of three domains along the proximal/distal axis: sheath (sh), auricle (au), and blade (bl). The ligule (li) normally develops at the sheath-auricle boundary on the adaxial side (left) and is absent from the abaxial side (right).
**(B)** to **(E)** Different domains of the wild-type leaf are distinguishable based on epidermal characteristics.
**(B)** Adaxial blade, showing macrohairs.
**(C)** Abaxial blade, lacking macrohairs.
**(D)** Adaxial sheath, which is not hairy.
**(E)** Abaxial sheath, which is hairy.
**(F)** *mwp1-R* mutants have an ectopic ligule at the sheath-auricle boundary as well as adaxialized sectors (red arrow) that extend below the ligule and above the node, sometimes with development of large laminar flaps (black arrow). The horizontal line marks the position of the section shown in **(G)**.
**(G)** Transverse section through a *mwp1* mutant sheath, showing ectopic cell proliferation and extra vascular bundles lacking the abaxial hypodermal sclerenchyma.
**(H)** Transverse section through the wild-type sheath.
**(I)** Single flaps (white arrow) often develop at the sheath margins.
**(J)** Scanning electron micrograph of the margin region, including a nonhairy margin flap (left) that develops adjacent to normal-looking hairy sheath (right).
**(K)** Close-up view of the flap epidermis showing absence of hairs.
**(L)** Transverse section across the tapered sheath margin of a wild-type leaf.
**(M)** Close-up view of a wild-type vascular bundle, showing adaxial (ad) xylem and abaxial (ab) phloem.
**(N)** Transverse section through the margin region of a *mwp1-R* mutant leaf, showing the true margin (blunt) and the ectopic margin (tapered).
**(O)** to **(Q)** Close-up views of *mwp1-R* vascular bundles, with xylem at a peripheral location, as in **(O)** and **(Q)**, or correctly oriented, as in **(P)**.
Bars = 500 μm in **(E)**, 1 mm in **(J)**, and 200 μm in all others.

the collateral arrangement of the vascular bundles in normal-looking parts of *mwp1* mutant and wild-type leaves (Figures 2M and 2P). The blunt shape of the true margin (Figure 2N), which is adaxialized, and the tapered shape of the ectopic margin, which has normal adaxial/abaxial polarity, may reflect a requirement for adaxial and abaxial cell types for proper margin development. Because the sheath margins are the last part of the leaf to differentiate (Sylvester et al., 1990; Scanlon, 2003), the distribution of adaxialized sectors in the sheath of *mwp1* mutants is likely to reflect a requirement for *mwp1* activity late in leaf development.

### Positional Cloning of *mwp1*

Using a mapping population of 600 individuals, we placed *mwp1* in bin 7.02, within a 0.65-centimorgan interval flanked by two polymorphic markers (AY109968 and umc1036) that reside in contig 309 of the agarose FPC physical map (7/19/05 release) (Figure 3A). Twelve markers in contig 309 detect sequences located on rice chromosome 9 in the same relative order (Figure 3A; see Supplemental Table 1 online). One of these markers was a sorghum genomic clone (SOG1743; accession number BH245825) with sequence similarity to members of the *KAN* gene family in *Arabidopsis* (Eshed et al., 2001; Kerstetter et al., 2001), suggesting that the *mwp1* interval contained a *KAN* gene. The two partial genomic sequences that most likely corresponded to the maize ortholog of the sorghum gene, AZM4_25886 and AZM4_123646, were found to be absolutely linked to the *mwp1* phenotype and could be amplified from BAC clones detected by the sorghum probe. Given the similarity between the *mwp1* and *kan* phenotypes, we pursued this gene as a candidate.

*mwp1-R* is thought to have originated spontaneously in crosses involving inbred lines and tropical land races. PCR amplification of the *KAN* candidate gene in *mwp1-R* plants yielded a band 1.8 kb larger than the one obtained from several wild-type strains tested, including the A188, B73, Mo17, W22, and A632 inbred lines. We cloned and sequenced this fragment and found an insertion within the small first intron, 13 bp downstream of the splice donor site (Figures 3B and 3C). Consistent with the spontaneous origin of *mwp1-R*, the inserted sequence seems to correspond to a retrotransposon, as it is flanked by identical 479-bp-long terminal repeats in direct orientation, each with the canonical TG-CA terminal nucleotides. The insertion caused the tandem duplication of four nucleotides at the insertion site (Figure 3C).

To isolate additional *mwp1* mutant alleles, we crossed *mwp1-R* to lines carrying *Mutator* (*Mu*) transposons. Two additional alleles, *mwp1-2* and *mwp1-3*, were identified in noncomplementation screens among ~28,000 F1 plants. To identify the insertion sites in these new alleles, we searched for *Mu* insertions using PCR, by combining *mwp1*-specific primers with a *Mu*-out primer. No insertion was present in the *mwp1-2* allele, but instead we found a 443-bp deletion that was absent from the progenitors (Figure 3B). The deletion in *mwp1-2* affects the first two exons; therefore, *mwp1-2* transcripts are expected to be mis-spliced. The resulting sequence is predicted to encode a nonfunctional protein lacking most of the conserved GARP domain and truncated by a premature stop codon. The *mwp1-3* allele was found to carry a *Mu* element inserted at the splice acceptor site of the first intron and thus is also expected to interfere with normal intron splicing. Combined, the lesions identified in three independently isolated alleles provide strong evidence that *mwp1* corresponds to this *KAN* gene.

### *mwp1* Encodes a Conserved KAN Transcription Factor

The *mwp1* transcriptional unit consists of six exons that encode a predicted protein of 477 amino acids with an estimated molecular mass of 48.36 kD (Figure 3B). Several polyadenylation sites were identified downstream of the stop codon using 3′ rapid amplification of cDNA ends (RACE). Although we failed to identify the 5′ untranslated region of *mwp1* by means of 5′ RACE, the position of the translation start site is supported by our RT-PCR results and by the high sequence similarity to barley (*Hordeum vulgare*) and switchgrass (*Panicum virgatum*) ESTs (accession numbers BI777239 and FE615893) and the rice (*Oryza sativa*) genome. The most similar sequence in rice belongs to a predicted gene, LOC_Os09g23200, which can be considered the ortholog of *mwp1* based on sequence identity and chromosomal synteny. The GARP domains of *mwp1* and LOC_Os09g23200 are identical and differ only in a single amino acid residue from those of the *Arabidopsis* KAN1 and KAN2 proteins.

Using RT-PCR, we found evidence for the transcriptional activity of *mwp1* in all tissues and organs tested, including seedlings, vegetative leaves, prophylls, husk leaves, ears, and immature tassel flowers (Figure 3D). BLAST searches detected three ESTs matching the 3′ untranslated region (BM500926, DW902148, and DW890724), two of which are from a cDNA library of laser capture microdissected shoot apical meristems (Emrich et al., 2007). No transcripts were detected by RT-PCR in *mwp1-R* mutant seedlings using primers flanking the insertion, but we managed to amplify chimeric transcripts in *mwp1-R*, originating within the insertion and extending into the 3′ part of the gene, by combining gene-specific primers with primers for the retrotransposon (Figure 3E). Mis-spliced transcripts, with various combinations of intronic and exonic sequences, were amplified in *mwp1-2* using primers flanking the deletion, as a result of the use of cryptic and normal splice sites (Figure 3E).

The rice genome encodes at least six members of the *KAN* family; the most similar paralog of LOC_Os09g23200 is LOC_Os08g33050. Our search for *KAN* genes among available B73 genomic and cDNA sequences indicates that the maize genome encodes at least three genes closely related to LOC_Os09g23200 and LOC_Os08g33050, indicating that the family has expanded during maize evolution. To clarify the phylogenetic relationship between *mwp1* and its closest homologs, we performed a phylogenetic analysis using the aligned nucleotide sequences encoding the GARP domains of LOC_Os09g23200 and LOC_Os08g33050 with those of *mwp1* and the two most similar genes in the maize genome (named Zm *KAN1* and Zm *KAN3*), which were identified in the sequence of the c0112F01 (chromosome 1) and c0072N10 (chromosome 4) BACs, respectively. Our analysis further supported that *mwp1* is an ortholog of LOC_Os09g23200 and suggests that *mwp1* represents a single-copy gene in the maize genome. By contrast, the two maize genes closest to *mwp1* are more similar to each other than to

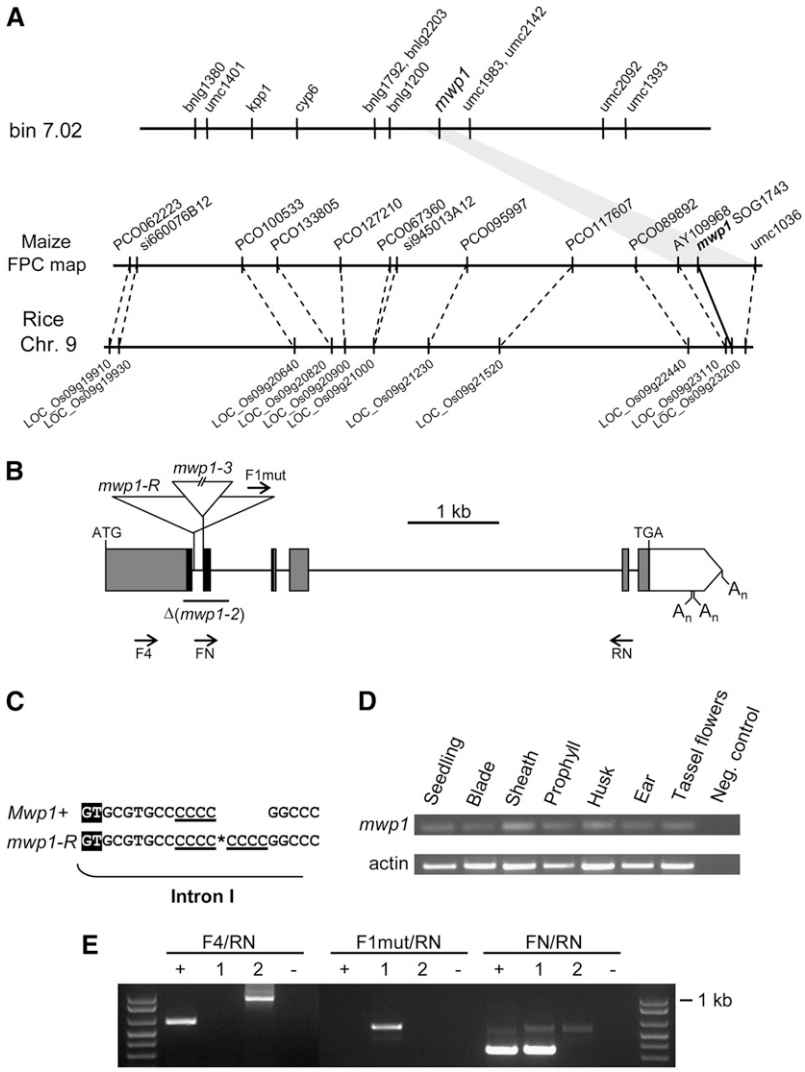


**Figure 3.** Molecular Cloning and Characterization of *mwp1* Alleles.

**(A)** Mapping strategy used to clone *mwp1*. *mwp1* was first mapped to bin 7.02 using molecular markers and subsequently assigned to an interval defined by markers AY109968 and umc1036 on a contig of the physical map with synteny to rice chromosome 9.

**(B)** Structure of the *mwp1* transcriptional unit, which consists of six exons (boxes) that encode an open reading frame (shaded boxes) with similarity to members of the KAN protein family. The sequence encoding the GARP domain characteristic of these proteins is in black. Triangles mark the insertions in the *mwp1-R* and *mwp1-3* alleles. The region deleted in the *mwp1-2* allele is indicated by a horizontal line. Arrows (not to scale) indicate the approximate position of some of the oligonucleotides used. $A_n$, polyadenylation sites.

**(C)** Duplication of four nucleotides at the insertion site of a retrotransposon in *mwp1-R*. A retrotransposon was found inserted at the site marked by an asterisk, 13 nucleotides downstream of the exon/intron boundary, and was flanked by a direct repeat of four nucleotides (underlined). The first two nucleotides (GT) of intron I are highlighted.

**(D)** RT-PCR analysis of *mwp1* expression in assorted tissues.

**(E)** RT-PCR analysis of *mwp1* expression in wild-type and mutant seedlings. Primers F4 and RN fail to amplify a band using cDNA from mwp1-R mutant seedlings but amplify larger products in *mwp1-2* due to mis-splicing. Primers F1-mut (specific to the *mwp1-R* insertion) and RN amplify a processed chimeric transcript only in *mwp1-R*, consisting of retrotransposon and gene sequences. Primers FN (which is specific to the region deleted in the *mwp1-2* allele) and RN amplify bands of the expected size using cDNA of wild-type and *mwp1-R* seedlings. Lanes correspond to the wild type (+), *mwp1-R* (1), *mwp1-2* (2), and water control (−). Molecular weight marker is 1 kb Plus (Invitrogen).

*mwp1* and LOC_Os08g33050, possibly representing a duplicate pair of genes (Figure 4; see Supplemental Figure 1 online). Trees with the same topology were obtained when the predicted full-length sequences of the proteins were used (data not shown). Previous authors have pinpointed additional regions in *KAN* proteins that are highly conserved across the dicotyledonous plants *Arabidopsis* and *Ipomoea* (Iwasaki and Nitasaka, 2006). These domains were also uncovered by our alignment of maize and rice sequences, suggesting that they are also important for KAN function in monocots (Figure 4A). Based on sequence comparisons of these domains, *mwp1* is most similar to *KAN1*.

### Expression Analysis of *mwp1* and *rld1*

In situ hybridization was performed to determine the tissue localization of *mwp1*. In wild-type seedlings, mRNA expression of *mwp1* was most intense in the abaxial epidermis of the sheath, clearly visible at plastochron 6 (P6) (Figures 5A and 5D). A similar trend was also observed in leaves that initiated later in development. In young leaf primordia (P1-3), expression was seen throughout the primordia, but more pronounced at the margins and in the vasculature (Figures 5F to 5I). The expression at the margin may reflect the requirement for *mwp1* activity inferred

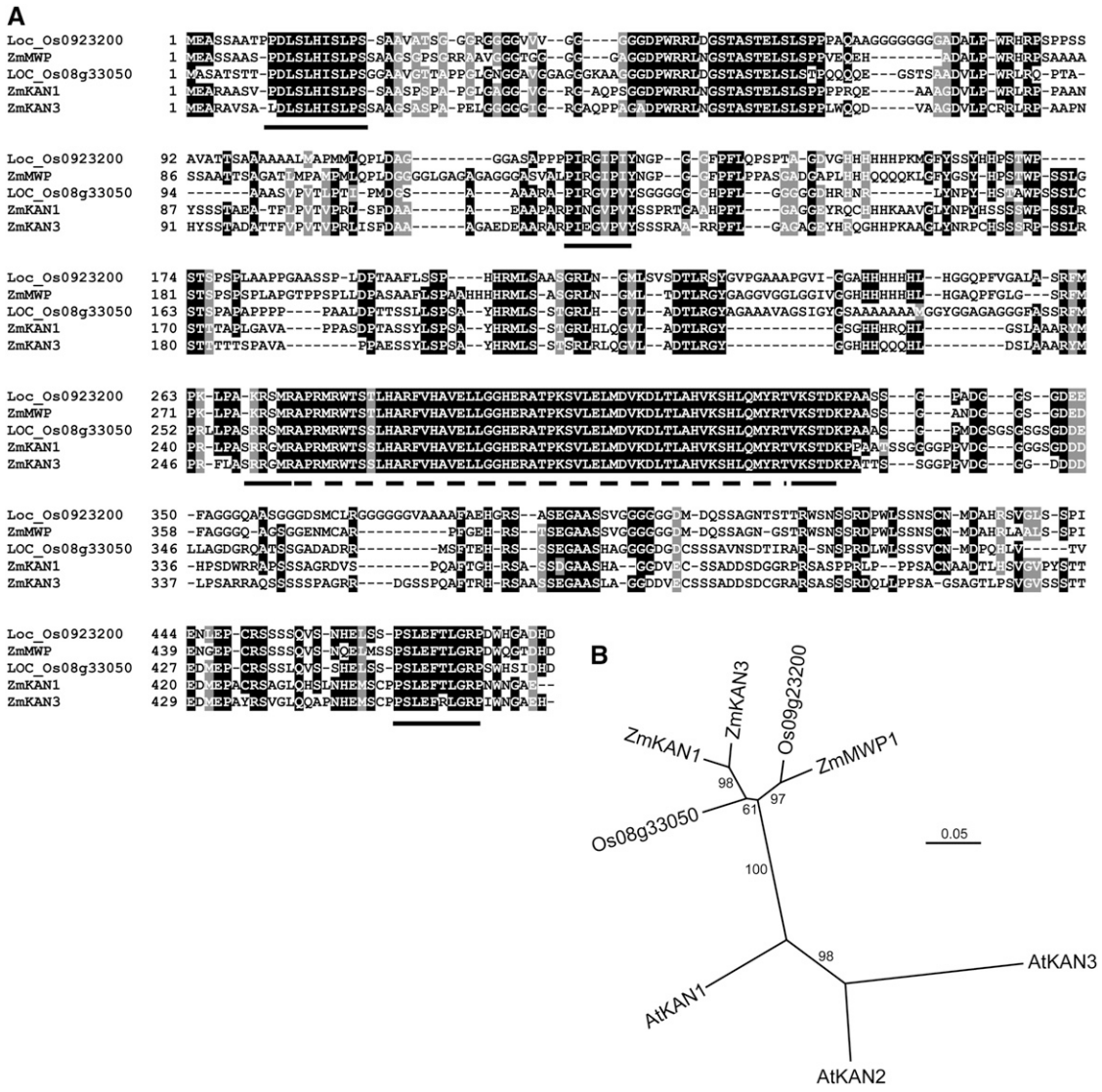


**Figure 4.** Sequence Alignment and Phylogenetic Analysis of *mwp1* and Related *KAN* Genes.

**(A)** Alignment of the amino acid sequences of mwp1 and the four most similar proteins in maize and rice. A dashed line indicates the GARP domain. Black lines indicate additional conserved regions in KAN proteins, first identified by Iwasaki and Nitasaka (2006), which are also conserved in KAN proteins from grasses.

**(B)** Neighbor-joining phylogenetic tree based on an alignment of the nucleotide sequence coding for the GARP domain. Numbers at the branches are percentages based on 10,000 bootstrap repetitions.

from the observed margin phenotypes (Figure 2I). Longitudinal sections showed that *mwp1* expression was absent from the apex of the meristem (Figures 5G and 5H), a region where *rld1* expression is high (Juarez et al., 2004b). Consistent with the expression patterns of *KAN* genes in *Arabidopsis* (Kerstetter et al., 2001), transverse sections showed reduced expression in the center of the meristem (Figure 5I). Expression was reduced, but not eliminated in *mwp1-2* (Figure 5B), which has a deletion but is not an RNA null (Figure 3E).

We also studied the expression of *mwp1* in dominant *Rld1-N1990* mutants, which carry a point mutation that disrupts the complementarity between *rld1* transcripts and the miR166 microRNA (Juarez et al., 2004b). In contrast with wild-type plants, *mwp1* transcripts were absent from the abaxial epidermis of *Rld1-N1990* mutants (Figures 5C and 5E), as expected if *rld1* is a direct or indirect negative regulator of *mwp1*.

The expression pattern of *rld1* (Juarez et al., 2004a, 2004b) was examined to determine if genes that are normally expressed adaxially are misexpressed in *mwp1* mutants. *rld1* was expressed on the adaxial side of wild-type husk leaf primordia and persisted at the margins and in vascular bundles (Figure 6A) in a pattern similar to that seen in vegetative leaves (Figure 6E).

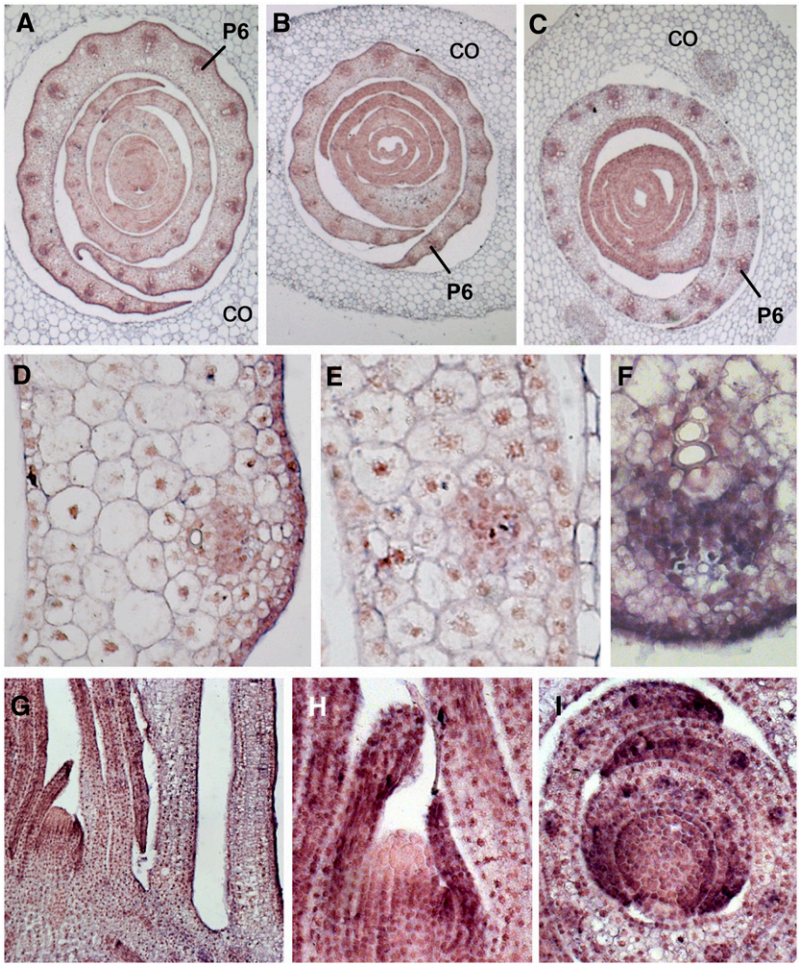


**Figure 5.** In Situ Hybridization Analysis of *mwp1* Expression.

**(A)** to **(C)** Transverse sections of young seedlings 2 d after germination, showing several developing leaves covered by the coleoptile (CO). The oldest (most external) leaf primordia are at plastochron 6 (P6) stage and were sectioned at the level of the sheath.
**(A)** Wild-type seedling.
**(B)** *mwp1-2* seedling.
**(C)** *Rld1-N1990* seedling.
**(D)** Magnified view of the sheath of a wild-type developing leaf, showing higher expression in the abaxial epidermis.
**(E)** Magnified view of **(C)** showing reduced expression in the abaxial epidermis.
**(F)** Close-up view of a wild-type vascular bundle showing *mwp1* expression between the xylem and phloem.
**(G)** Longitudinal section of a wild-type shoot apical meristem and the surrounding leaf primordia.
**(H)** Close-up view of the meristem in **(G)**. Expression is absent from the apex of the meristem.
**(I)** Transverse section of a wild-type shoot apical meristem showing strong expression in the margins of P2 and P3 leaf primordia.

Ectopic outgrowths on the abaxial side of developing *mwp1* husk leaves were associated with *rld1* misexpression (Figures 6B to 6D). In the region delimited by the outgrowths, *rld1* was expressed both adaxially and abaxially, with strong expression in the abaxial epidermis (Figures 6C and 6D). *rld1* expression was also examined in *mwp1-R* leaf primordia with developing sheath margin outgrowths. In the wild type, *rld1* was expressed on the adaxial side of young leaf primordia. Expression persisted at the margins and in developing vascular bundles of older primordia (Figure 6E). However, in *mwp1-R* leaves, *rld1* expression was seen throughout the sheath margin (Figures 6F and 6G). The boundary between *rld1*-expressing and nonexpressing tissues corresponded to the position of the developing outgrowth. These results suggest that the expression of *mwp1* at the abaxial margin is required to keep *rld1* restricted to the adaxial margin, the loss of *mwp1* function leading to a pronounced defect in this location (Figures 2I and 2N).

### The Phenotype of *Rld1/rld+; mwp1* Double Mutants Is Synergistic

To further investigate the functional relationship between *mwp1* and *rld1*, we analyzed the double mutant. *Rld1* mutants are characterized by upwardly curving leaf blades and by the presence of patches of ligule (Figure 7A), macrohairs, and bulliform cells (arrow in Figure 7K) on the abaxial side of the leaf (Nelson et al., 2002; Juarez et al., 2004b). In addition, small sectors of pale green tissue lacking the minor vasculature have been reported in the blade and the sheath (Nelson et al., 2002).

The *Rld1-N1990/rld+; mwp1-R* double mutants had husk leaves with outgrowths similar to those of *mwp1-R* single mutants (data not shown). In addition, a new phenotype consisting of broad longitudinal sectors of nonphotosynthetic tissue flanked by laminar flaps was consistently observed on the abaxial side of the uppermost vegetative leaves (Figures 7B to 7D). These pale sectors were often positioned at paired, bilaterally symmetric locations on both sides of the midrib and extended along the entire sheath and most of the blade, where they were narrower but still flanked by flaps (Figure 7D). The sectors continued from leaf to leaf, suggesting that they originated in the meristem and maintained their fate through subsequent cell divisions. Sectors in consecutive leaves were connected by internode sectors with slightly lighter pigmentation, in which the vasculature failed to appress to the stem surface (see Supplemental Figure 2 online). Occasionally, laminar growth associated with these sectors gave rise to leaf-like organs fused at the sheath of the leaf from which they originated, detaching distally and differentiating into a blade and an auricle (Figure 7C). In addition, one or two nodes immediately below the lowest tassel branch were occasionally leafless, their leaves being replaced by membranous ligule-like outgrowths (Figure 7B).

To understand the nature of these sectors, cell types in the double mutant were analyzed and compared with those of the wild type. The abaxial side of the sheath was covered by hairs, as in the wild type, except at the sector where the epidermis was hairless and consisted of brick-shaped, rectangular cells and rows of stomatal complexes, resembling the epidermis of the adaxial side (Figures 7E and 7F). Occasionally, small prickle-like hairs, similar to those seen in adaxial husk leaves, were visible in the sectors (right-hand side of Figure 7G). These differed from the longer hairs in the flanking abaxial sheath (left-hand side of Figure 7G). In general, the phenotype of the *Rld1-N1990/rld+*

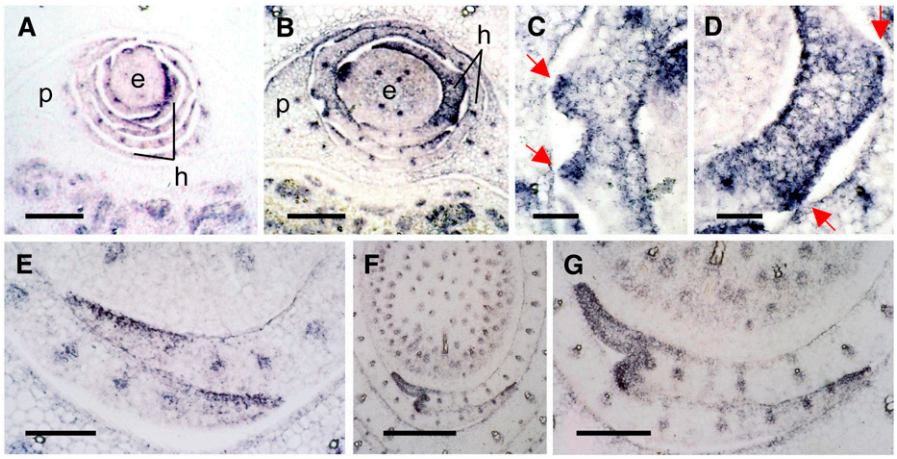


**Figure 6.** In Situ Hybridization Analysis of *rld1* Expression in Wild-Type and *mwp1* Plants.

**(A)** and **(B)** Transverse sections of female axillary shoots, showing the developing ear (e) covered by several husk leaves (h) and a prophyll (p).
**(A)** The wild type.
**(B)** *mwp1-R* showing ectopic abaxial expression of *rld1* in the husk leaves associated with developing pairs of leaf flaps.
**(C)** and **(D)** Magnified views of the developing flap pairs in **(B)**. The pairs of flaps in are indicated by red arrows.
**(E)** Wild-type vegetative leaf margins showing adaxial *rld1* expression.
**(F)** *mwp1-R* vegetative leaves showing ectopic *rld1* expression and a developing margin flap.
**(G)** Magnified view of **(F)**.
Bars = 50 μm in **(C)** and **(D)**, 500 μm in **(F)**, and 200 μm in all others.

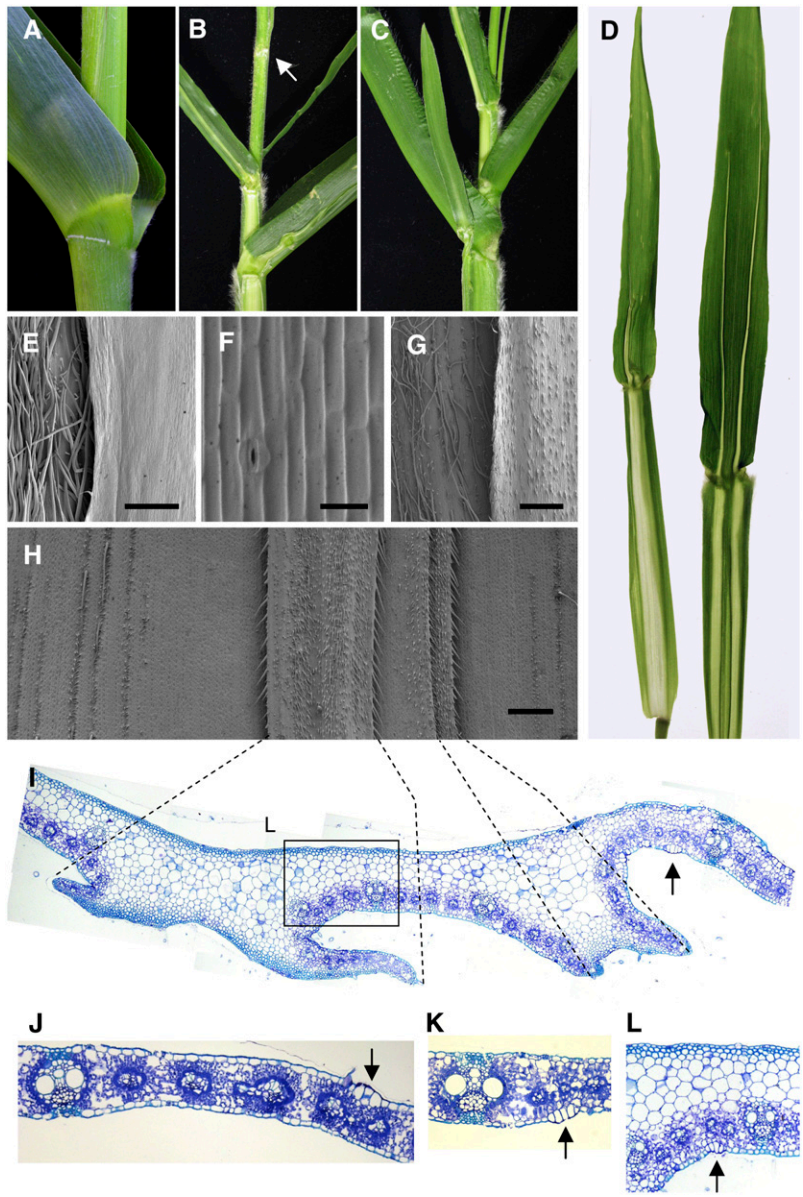


**Figure 7.** The Synergistic Phenotype of *mwp1*; *Rld1* Double Mmutants.

**(A)** *Rld1-N1990/rld1+* mutant.
**(B)** *mwp1-R*; *Rld1-N1990/rld1+* double mutant showing longitudinal sectors that extend the length of sheath and blade. A leafless node is indicated by a white arrow.
**(C)** Same genotype as in **(B)** but with an ectopic blade fused to and developing from a sector in the main leaf.
**(D)** *mwp1-R*; *Rld1-N1990/rld1+* double mutant leaves extended to show the shape and propagation of the sectors from sheath to blade.
**(E)** Scanning electron micrograph of the sheath of a *mwp1-R*; *Rld1-N1990/rld1+* mutant leaf, as seen from the abaxial side, showing normal-looking sheath (left side) and the adaxialized, hairless epidermis of a sector (right side).
**(F)** Magnified view of the adaxialized epidermis of the sector shown in **(E)**.
**(G)** Sheath of *mwp1-R*; *Rld1-N1990/rld1+* mutant leaf showing an adaxialized sector with small hairs (right side), in contrast with the hairy, normal-looking sheath of adjacent tissue.
**(H)** Scanning electron micrograph of the sectors and flaps observed on the abaxial surface of *mwp1-R*; *Rld1-N1990/rld1+* leaf blades.
**(I)** Transverse section corresponding to the region shown in **(H)**. Dashed lines connect equivalent positions in **(H)** and **(I)**, corresponding to developing ectopic blade margins.
**(J)** Transverse section of an *mwp1-R* leaf that, like the wild type, shows bulliform cells only on the adaxial epidermis (arrow).
**(K)** Transverse section of a *Rld1-N1990/rld1+* leaf, showing bulliform cells (arrow) on the abaxial side but not on the adaxial.
**(L)** Detailed view of **(I)**, showing abaxial bulliform cells (arrow) as in **(K)**.

*mwp1-R* sheath was similar to that of the *mwp1-R* husk leaves. By contrast, most of the blade epidermis resembled that of *Rld1-N1990/rld+* single mutants; broad areas of the epidermis showed reversed polarity, with macrohairs and bulliform cells on the abaxial surface but not on the adaxial surface (Figures 7H and 7L). Regions with reversed polarity were often intermixed with regions of normal polarity. Transverse sections through the blade sectors revealed thickened areas with symmetrically organized internal tissues and a complete absence of photosynthetic and vascular tissues (Figure 7I). Bulliform cells could be seen on the abaxial side immediately adjacent to the flaps (Figure 7L, arrow), suggesting that these cells were adaxialized. However, adjacent to these bulliform cells were areas in which macrohairs were correctly patterned: absent from the abaxial side (see hairless area surrounding the flaps in Figure 7H) and present on the adaxial side (data not shown). The abaxial surface of blade sectors themselves was covered by small hairs and, sometimes, macrohairs, suggesting that they in fact originated from adaxialization of tissues within the sector. The presence of adaxial features within the sector suggests that the juxtaposition of this localized adaxialization within a region of abaxial identity led to formation of flaps. In summary, the double mutant phenotype appears to be synergistic as the sectors of adaxialization extend the entire length of the leaf and go from leaf to leaf as if they originated in the meristem. Within the sectors, certain tissues are not simply adaxialized, but fail to differentiate at all.

## DISCUSSION

*mwp1-R* is a recessive mutant characterized by sectors of adaxialized tissue in the sheath domain of vegetative and husk leaves. The mutant phenotype suggests a role for *mwp1* in the initiation and/or maintenance of abaxial identity. We cloned *mwp1* by following a positional approach and found that it encodes a member of the KAN family of GARP transcription factors. In *Arabidopsis*, *KAN* gene expression marks the abaxial side of leaves and the peripheral region of the meristem (Kerstetter et al., 2001). Similarly, we found *mwp1* expressed in the abaxial epidermis, consistent with a function in promoting abaxial identity and repressing adaxial identity. Although *mwp1* transcripts were found in sheath and blade, we only observed adaxialization in the sheath of *mwp1* mutant leaves. In *Arabidopsis*, similar severe phenotypes are only observed in double or triple *kan* mutant combinations. The observation of a mutant phenotype in *mwp1* single mutants suggests that some *KAN* genes have evolved unique functions in grass leaves and therefore are not as functionally redundant as their *Arabidopsis* counterparts.

The *mwp1* phenotype was particularly evident in husk leaves, with pairs of flaps that often extended the entire sheath length. In *Arabidopsis*, disorganized growth, expansion of the blade in various planes, or development of ectopic leaf-like organs have been reported for *kan1 kan2* (Eshed et al., 2001) and *kan1 kan2 kan4* triple mutants (Izhaki and Bowman, 2007), but their compromised development made interpretation of the phenotypes difficult in terms of local changes in abaxial/adaxial polarity. Our observations of *mwp1* husk leaves allow a clearer interpretation of the phenotype and demonstrate that new planes of laminar growth develop at the sites where the adaxialized sectors and the surrounding abaxial tissue juxtapose. According to the model of Waites and Hudson (1995), a pair of ectopic leaf flaps develops when sectors with adaxial identity are flanked on both sides by cells with abaxial identity (Figure 8A). A similar model can be applied to the single leaf flaps at the sheath margin. The loss of abaxial identity at the margin generates only one new boundary between abaxial and adaxial cells and thus only one ectopic flap develops (Figure 8B). Despite the absence of morphological markers in *Arabidopsis*, the ectopic expression of a leaf margin reporter in the abaxial outgrowths of *kan1 kan2* double mutants suggests that a similar mechanism operates in *Arabidopsis* (Eshed et al., 2004).

The sectored nature of the *mwp1* phenotype shows that the shift from abaxial to adaxial identity occurs locally, rather than in the sheath as a whole. The polar (along the proximal/distal axis) orientation of the *mwp1* defects raises the possibility that they originate from a local failure in the maintenance or initiation of abaxial fate that is subsequently propagated clonally as leaf cells proliferate. A failure in maintaining stable transcriptional states through mitosis was also hypothesized as the cause for the mosaicism seen in other mutants, as in the *incurvata2* (*icu2*) mutants of *Arabidopsis*, which ectopically express the floral identity gene *AGAMOUS* in leaf sectors (Serrano-Cartagena et al., 2000). Cloning of *ICU2* has shown that it encodes a DNA polymerase $\alpha$-subunit that physically interacts with other proteins involved in chromatin-mediated gene repression (Barrero et al., 2007). Interestingly, the abaxial outgrowths in *kan1 kan2* double mutants are suppressed by loss-of-function alleles of the SWI/SNF gene *SPLAYED* in *Arabidopsis* (Eshed et al., 2004), possibly reflecting the participation of a mechanism of cellular memory that involves chromatin remodeling.

In vegetative leaves, the sheath responds to loss of *mwp1* function in a different way. The adaxializing effect of *mwp1* mutations is clearly shown by the development of ectopic ligules on the abaxial side. The location of such ectopic ligules at the sheath-auricle boundary indicates that the site of ligule development is specified by a combination of positional cues from the proximal/distal and the abaxial/adaxial axes. In addition, leaf flaps appeared at various locations, including the proximal end of the sheath, below the ectopic ligules, and along the sheath margin. In many cases, however, the shape, internal organization, and distribution of these sectors seem incompatible with their origin from a single, clonally propagated event. The possible involvement of a mechanism of epigenetic silencing, however, is supported by the observation of adaxialized phenotypes strikingly similar to those of *mwp1-R* in mutants such as *required to maintain repression6* (Parkinson et al., 2007) and *mediator of paramutation1* (D. Lisch, personal communication), both of which fail to maintain stable epigenetic states during paramutation. A mosaic analysis previously showed that non-cell autonomous signals from *Rld1* mutant sectors trigger a reversal of polarity in the underlying wild-type cell layers (Nelson et al., 2002). Further clonal and mosaic analyses will be required to understand whether the sectoring in *mwp1* mutants is clonal or involves cell-to-cell communication.

Given that maize leaves elaborate and differentiate from the tip to the base and from the midrib to the margin (Sharman, 1942; Sylvester et al., 1990; Scanlon, 2003), it appears that the *mwp1*

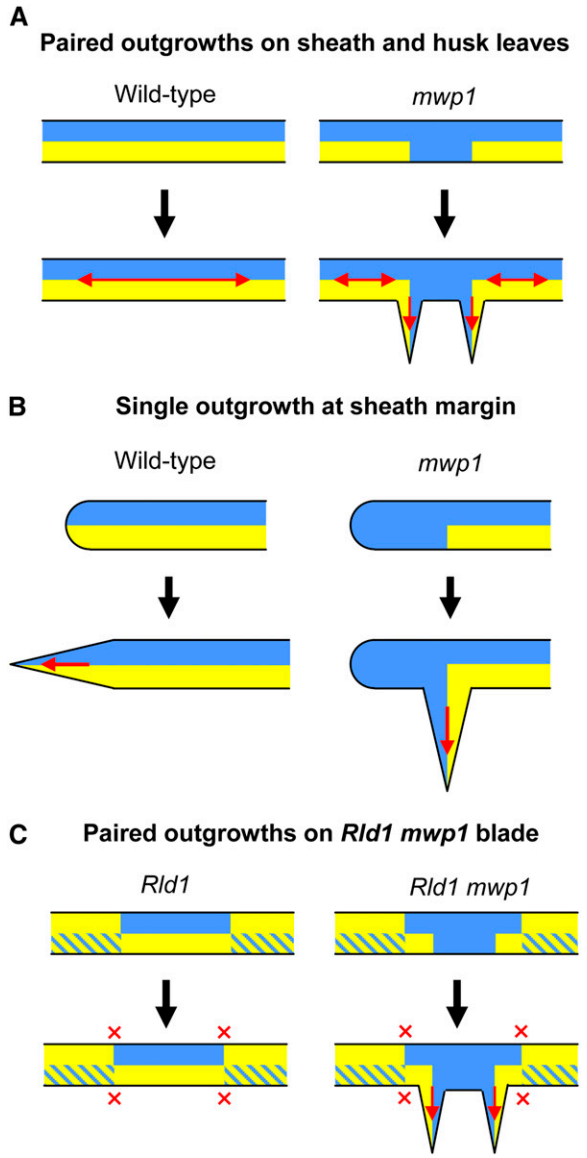


**Figure 8.** Model for the Development of Laminar Outgrowths in *mwp1* Mutants and in *mwp1*; *Rld1* Double Mutants.

**(A)** In wild-type husk leaves, the juxtaposition of adaxial (blue) and abaxial (yellow) cell types promotes laminar growth (red arrows). In *mwp1* leaves, a failure to initiate or maintain abaxial identity in husk leaves results in ectopic adaxial cell types on the adaxial side, creating new boundaries of juxtaposed abaxial and adaxial identity. As predicted by the juxtaposition model, growth then occurs at the planes defined by these new boundaries.

**(B)** When ectopic adaxial cell types are present at the sheath margin, a single ectopic boundary is created, resulting in the development of a single outgrowth.

**(C)** *Rld1* mutations often cause a complete switch in the abaxial/adaxial polarity of the blade. Sectors with normal polarity are often located adjacent to sectors with reversed polarity, but this juxtaposition does not normally lead to laminar outgrowths (red crosses). Development of outgrowths in *mwp1*; *Rld1* blades may occur in response to adaxialization in sectors of the blade that otherwise retain abaxial identity on the abaxial side.

defect becomes more pronounced in tissues that differentiate late. In tissues that differentiate early, either no defect is seen (in blade and at midrib) or minor defects are seen (at the top of the sheath). Consistent with a role for *mwp1* in tissues that differentiate late in leaf development, we also see a similar trend within the plant as a whole. The *mwp1* mutant phenotype is not seen in juvenile leaves and becomes more severe in leaves that form late in the life of the maize plant, which includes the husk leaves that are initiated during the reproductive state.

Despite the fact that *mwp1-R* and *Rld1* mutations both result in adaxialized leaf phenotypes, they differ in the specificity of their effects on sheath and blade, respectively. The anatomy of the sheath remains unaffected in *Rld1* mutants, but the blade exhibits a distinct upward curling and an altered distribution of hypodermal sclerenchyma, bulliform cells, and macrohairs, all of which are characteristically patterned along the abaxial-adaxial axis in normal leaves (Nelson et al., 2002; Juarez et al., 2004b). Although the *Rld1* epidermis has juxtaposed abaxial and adaxial cell identities, as determined by the presence of macrohairs, no flaps occur. In contrast with *Rld1* mutants, we did not observe changes in the anatomy of the blade in *mwp1* mutants, despite the range of mutant phenotypes present in the sheath. Outgrowths were consistently observed in the sheath of *mwp1* mutants at the sites where abaxial and adaxial identities juxtapose but have not been reported in the sheath or the blade of *Rld1* mutants or flanking the boundaries of *rld1*+ sectors in *Rld1* mosaic plants (Nelson et al., 2002). Thus, *Rld1* and *mwp1* mutants also differ in their ability to initiate new axes of growth in leaves.

Double mutants of *mwp1-R* and *Rld1-N1990* showed a synergistic phenotype in which the sectors and paired flaps characteristic of *mwp1*, normally confined to the sheath domain, extend outside the sheath and into the blade. These flaps occur in a tissue that is already adaxialized. A plausible explanation for these flaps is that the *mwp1* mutation affects the abaxial identity in regions of the blade that have maintained normal polarity (Figure 8C). The sectors observed in *mwp1; Rld1* double mutants have adaxial features on both surfaces but appear to be flanked on the abaxial surface by normal abaxial cell types.

The expansion of the *mwp1* defect into the blade in an *Rld1* mutant background may be due to a redundant *KAN* gene functioning in the blade in *mwp1-R* mutants. At least two other *KAN* genes, Zm *KAN1* and Zm *KAN3*, are expressed in blade tissue (see Supplemental Figure 3 online). With such a scenario, both *KAN* genes would be repressed by ectopic *HD-ZIPIII* expression in *Rld1* mutants. *Rld1* single mutants have clearings observed above and below the blade-sheath boundary, which are pale green and fail to develop intermediate and transverse veins (Nelson et al., 2002). The sectors observed in *mwp1; Rld1* double mutants most likely represent an enhancement of these clearings as a consequence of increased *rld1* expression or a change in the timing or domain of expression beyond what is seen in *Rld1* single mutants. Although previous results have suggested that *Rld1* mutations behave as antimorphic or dominant-negative alleles (Nelson et al., 2002), molecular data suggest that dominant *Rld1* alleles are best described as hypermorphic or neomorphic. If this is actually the case, the molecular basis of the observed enhancement may lie at the titration of ZPR proteins (Wenkel et al., 2007; Kim et al.,

2008) by increased RLD1 levels, causing increased adaxialization in double mutants.

The timing of polarity establishment is likely to be critical for vascular development. The adaxialized sectors in *mwp1; Rld1* double mutants demonstrate that initiation of vasculature and differentiation of photosynthetic mesophyll cells cannot proceed without abaxial identity or without the formation of adaxial-abaxial boundaries. These sectors are likely to originate early in leaf initiation, since they continue for the length of the leaf and appear to go from leaf to leaf. Their position in the leaf between the midrib and the margin may indicate a particular domain of the leaf, such as that defined by *narrow sheath* (Scanlon, 2000) or *Wavy auricle in blade1* (Hay and Hake, 2004). By contrast, the sectors of *mwp1* single mutants are confined to the sheath and do not go from leaf to leaf. Thus, correct polarity regulated by MWP1 and RLD1 is needed early in leaf development to create vasculature and later in leaf development to maintain cell identity and prevent new lamina from forming.

Other authors have proposed a dual abaxializing and adaxializing function for *KAN* genes based on the abaxialized vasculature seen in the petioles of some *kan1 kan2* double mutants (Ha et al., 2007). One attractive possibility is that normal development in distinct leaf domains (petiole/blade in *Arabidopsis* or sheath/blade in maize) involves the same developmental pathways but a different interpretation of positional information. In line with this idea, it is remarkable that sheath and blade of normal maize leaves exhibit reciprocal patterns of hairiness on their adaxial and abaxial surfaces. One might also speculate as to whether the absence of laminar growth in the petioles of *Arabidopsis* rosette leaves is attained by regulating abaxial-adaxial patterning. Further research on the adaxial-abaxial patterning mechanisms might therefore contribute to advance our understanding of the morphogenesis of differently shaped leaf domains.

## METHODS

### Plant Materials

The *mwp1-R* allele was obtained from the Maize Genetics Cooperation Stock Center (accession number 5804F; http://maizecoop.cropsci.uiuc.edu/) and backcrossed at least four times to several inbreds, including B73, A632, W23, and A188. An *Rld1-N1990* mutant line that had been backcrossed twice to W23 was also obtained from the stock center (accession number 927K). Double mutants were identified in the F2 generation of a cross of this line and *mwp1-R*. The *Rld1-N1990*/*rld1*+; *mwp1-R* double mutant has since been maintained by repeated backcrossing to *mwp1-R* mutant introgressed in W23. Plants were grown in our Gill Tract summer nursery or in the greenhouse for phenotypic and molecular studies in Albany, CA.

### Isolation of *mwp1-2* and *mwp1-3*

Two additional alleles were identified in the F1 progeny of crosses of females carrying active *Mu* elements and *mwp1-R* males. F1 plants were field grown and screened either in the Gill Tract or at the University of Illinois at Urbana-Champaign. Putative mutants were crossed to one or more inbred lines, and their F1 progenies self-pollinated to establish F2 families segregating either *mwp1-R* or the newly induced allele. *mwp1-2* was outcrossed to several inbred backgrounds for four generations. No families segregating the *mwp1-3* allele have been found, suggesting a transmission problem or that the insertion in the original mutant was somatic. However, we managed to amplify a *Mu* insertion in *mwp1-3* using DNA purified from mutant tissue collected at the time of the screen.

### Mapping and Characterization of Alleles

Genetic linkage was first detected between *mwp1-R* and the visible *Rough sheath1* mutant, which maps to chromosome 7, in a family segregating both traits. Linkage to chromosome 7 was then confirmed using bulked segregant analysis (Michelmore et al., 1991) of simple sequence repeat markers and subsequently tested on individual plants. Our mapping population was the progeny of a testcross segregating *mwp1* and wild-type plants in a 1:1 ratio. Information on the simple sequence repeat markers used (shown in Figure 3) is available from the MaizeGDB website (http://www.maizegdb.org). We identified additional single nucleotide polymorphisms in genes previously localized in the maize FPC physical map (http://www.genome.arizona.edu/fpc/WebAGCoL/maize/WebFPC/) or in genes selected based on the synteny with the rice genome, which were likely to map to the candidate interval. Such single nucleotide polymorphic markers were scored by direct sequencing of PCR fragments spanning the polymorphism, using an ABI 3100 genome analyzer and BigDye Terminator v3.1 cycle sequencing chemistry (Applied Biosystems).

For characterizing the alleles, primers were designed to amplify the genomic region defined by the AZM4_25886 and AZM4_123646 contigs and to bridge the gap between them. Two such primers, mwp-F4 (5′-CTGCCAATCCGAGGGATAC-3′) and mwp-R4 (5′-TTTCATTCACCGTCTGGAGTT-3′), amplified a bigger fragment when genomic DNA of *mwp1-R* was used as the template. The same primers detected a smaller fragment in *mwp1-2*. The *Mu* insertion of the *mwp1-3* allele was detected by PCR combining gene-specific primers with Pioneer's 9242 *Mu*-specific degenerate primer (5′-AGAGAAGCCAACGCCAWCGCCTCYATTTCGTC-3′) (Blauth et al., 2001).

### Light Microscopy

For plastic sections, the tissue was fixed overnight in FAA (50% ethanol, 5% acetic acid, and 3.7% formaldehyde), dehydrated through a series of increasing ethanol concentration, and embedded in Technovit 7100 according to the manufacturer's instructions (Heraeus Kulzer). Alternatively, the tissue was fixed in a solution containing 2% glutaraldehyde and 2% paraformaldehyde in 0.1 M phosphate buffer and embedded in Procure 812 (ProSciTech). Sections of 1 to 4 μm thickness were cut using an HM340 microtome (Microm), stained with 0.05% (w/v) Toluidine blue O, rinsed with water, allowed to dry, mounted on slides with Permount (Fisher Scientific), and photographed in a bright-field microscope.

### Scanning Electron Microscopy

For scanning electron microscopy, plant tissue was fixed overnight as described above, dehydrated with ethanol, and critical-point dried with liquid $CO_2$. Samples were then coated with gold palladium using a Desk II sputter coater (Denton Vacuum) for 45 s and examined on a Hitachi S-4700 scanning electron microscope. Alternatively, samples were coated with 25-nm gold using a Polaron E 5400 sputter coater (SCD-050; Bal-Tec) and examined on a Cambridge 250 Mark III scanning electron microscope (Cambridge InstrumentsK).

### Gene Expression Analysis

Total RNA was purified from the aboveground, green parts of 2-week-old seedlings of the B73 inbred line using Trizol reagent according to the

manufacturer's instructions (Invitrogen). For 3′ RACE, RNA was treated with the GeneRacer RACE Ready cDNA kit and reverse transcribed with SuperScriptIII reverse transcriptase and the kit's oligo(dT) primer according to the manufacturer's instructions (Invitrogen). The resulting cDNA was used in nested PCR reactions with the gene-specific 3RACE-1F (5′-GGCTGTCGTCGAATTCATGCAACA-3′) and 3RACE-2F (5′-GCAGCCCGAGCCTGGAGTTCAC-3′) primers, which were combined with the GeneRacer 3′ and GeneRacer 3′ nested primers from the kit. The resulting bands were extracted from the gel, cloned into pGEM-T Easy (Promega), and sequenced to determine the position of the polyadenylation sites. For RT-PCR amplification of wild-type and mutant transcripts, the mwp1-F4 (see above), mwp1-RT-FN (5′-CATGGACGTGAAGGATCTGACC-3′), and mwp1-Fmut (5′-GGGGAATACAAGGGTCCAGT-3′) forward primers were combined with the mwp1-RT-RN (5′-GATGAGCATCCATGTTGCATGA-3′) reverse primer.

### Phylogenetic Analysis

Alignments of predicted full-length amino acid sequences were done automatically using MUSCLE software (Edgar, 2004) and subsequently refined manually. Alignments were also done with the segment of the nucleotide sequence that encodes the conserved GARP domain. Consensus phylogenetic trees were constructed for the aligned sequences with MEGA version 3.1 (Kumar et al., 2004) using the neighbor-joining and minimum evolution methods. Bootstrap values in the bootstrap consensus tree were produced with 10,000 replications.

### In Situ Hybridization

In situ hybridization was performed using the method of Jackson (1991), as modified by Bortiri et al. (2006). To generate a probe, a fragment of the first exon upstream of the GARP domain was amplified with mwp-probe-F (5′-GAGGGTGTCGGTGAGCAT-3′) and mwp-probe-R (5′-GAACGGGAGGAGGAGGAG-3′) primers and cloned into pGEM-T Easy (Promega).

### Accession Numbers

Sequence data from this article can be found in the GenBank/EMBL data libraries under the following accession numbers: BAC clone c0112F01 (AC199826), BAC clone c0072N10 (AC184836), *mwp1* cDNA (EU925398), *KAN1* cDNA (EU935003), and *KAN3* (EU925399).

### Supplemental Data

The following materials are available in the online version of this article.

**Supplemental Figure 1.** Alignment of Nucleotide Sequences.

**Supplemental Figure 2.** Cross Section of *Rld1; mwp1* Double Mutant Stem.

**Supplemental Figure 3.** RT-PCR Analysis of *KAN1* and *KAN3* Expression in Maize.

**Supplemental Table 1.** Maize-Rice Synteny for Selected Markers in Contig 309.

**Supplemental Data Set 1.** Alignment of Protein Sequences (from Figure 4A).

**Supplemental Data Set 2.** Alignment of Nucleotide Sequences (Used for the Tree in Figure 4B).

## ACKNOWLEDGMENTS

This work was supported by grant NSF IOS 0445387 and USDA–Agricultural Research Service funding to S.H. and a Marsden grant to T.F. (HRT0501) from the Royal Society of New Zealand. H.C. was a recipient of a postdoctoral fellowship of the Ministerio de Educación y Ciencia of Spain and R.J. of a FRST Bright Futures Scholarship. We thank Torbert Rocheford for field space, Marty Sachs and the Maize Genetics Cooperation Stock Center for maize strains, David Hantz and Julie Calfas for greenhouse support, Delilah F. Wood and Tina Williams for the use of the electron microscopy facility, Doug Hopcroft and Raymond Bennett for assistance with scanning electron microscopy, and Marja Timmermans for providing the *rld1* probe. We also wish to acknowledge the helpful discussions and editing from lab members.

Received March 28, 2008; revised July 15, 2008; accepted July 31, 2008; published August 29, 2008.

## REFERENCES

**Bao, N., Lye, K.W., and Barton, M.K.** (2004). MicroRNA binding sites in Arabidopsis class III HD-ZIP mRNAs are required for methylation of the template chromosome. Dev. Cell **7:** 653–662.

**Barrero, J.M., Gonzalez-Bayon, R., del Pozo, J.C., Ponce, M.R., and Micol, J.L.** (2007). *INCURVATA2* encodes the catalytic subunit of DNA polymerase alpha and interacts with genes involved in chromatin-mediated cellular memory in *Arabidopsis thaliana*. Plant Cell **19:** 2822–2838.

**Blauth, S.L., Yao, Y., Klucinec, J.D., Shannon, J.C., Thompson, D.B., and Guilitinan, M.J.** (2001). Identification of *Mutator* insertional mutants of starch-branching enzyme 2a in corn. Plant Physiol. **125:** 1396–1405.

**Bortiri, E., Chuck, G., Vollbrecht, E., Rocheford, T., Martienssen, R., and Hake, S.** (2006). *ramosa2* encodes a LATERAL ORGAN BOUNDARY domain protein that determines the fate of stem cells in branch meristems of maize. Plant Cell **18:** 574–585.

**Edgar, R.C.** (2004). MUSCLE: A multiple sequence alignment method with reduced time and space complexity. BMC Bioinformatics **5:** 1–19.

**Emery, J.F., Floyd, S.K., Alvarez, J., Eshed, Y., Hawker, N.P., Izhaki, A., Baum, S.F., and Bowman, J.L.** (2003). Radial patterning of Arabidopsis shoots by class III HD-ZIP and KANADI genes. Curr. Biol. **13:** 1768–1774.

**Emrich, S.J., Barbazuk, W.B., Li, L., and Schnable, P.S.** (2007). Gene discovery and annotation using LCM-454 transcriptome sequencing. Genome Res. **17:** 69–73.

**Esau, K.** (1960). Anatomy of Seed Plants. (New York: Wiley).

**Eshed, Y., Baum, S.F., and Bowman, J.L.** (1999). Distinct mechanisms promote polarity establishment in carpels of Arabidopsis. Cell **99:** 199–209.

**Eshed, Y., Baum, S.F., Perea, J.V., and Bowman, J.L.** (2001). Establishment of polarity in lateral organs of plants. Curr. Biol. **11:** 1251–1260.

**Eshed, Y., Izhaki, A., Baum, S.F., Floyd, S.K., and Bowman, J.L.** (2004). Asymmetric leaf development and blade expansion in Arabidopsis are mediated by KANADI and YABBY activities. Development **131:** 2997–3006.

**Evans, M.M.** (2007). The *indeterminate gametophyte1* gene of maize encodes a LOB domain protein required for embryo Sac and leaf development. Plant Cell **19:** 46–62.

**Ha, C.M., Jun, J.H., Nam, H.G., and Fletcher, J.C.** (2007). *BLADE-ON-PETIOLE 1* and *2* control Arabidopsis lateral organ fate through regulation of LOB domain and adaxial-abaxial polarity genes. Plant Cell **19:** 1809–1825.

**Hay, A., and Hake, S.** (2004). The dominant mutant *Wavy auricle in blade1* disrupts patterning in a lateral domain of the maize leaf. Plant Physiol. **135:** 300–308.

**Henderson, D.C., Muehlbauer, G.J., and Scanlon, M.J.** (2005). Radial leaves of the maize mutant *ragged seedling2* retain dorsiventral anatomy. Dev. Biol. **282:** 455–466.

**Henderson, D.C., Zhang, X.L., Brooks, L., and Scanlon, M.J.** (2006). RAGGED SEEDLING2 is required for expression of KANADI2 and REVOLUTA homologues in the maize shoot apex. Genesis **44:** 372–382.

**Iwasaki, M., and Nitasaka, E.** (2006). The *FEATHERED* gene is required for polarity establishment in lateral organs especially flowers of the Japanese morning glory (*Ipomoea nil*). Plant Mol. Biol. **62:** 913–925.

**Izhaki, A., and Bowman, J.L.** (2007). KANADI and class III HD-Zip gene families regulate embryo patterning and modulate auxin flow during embryogenesis in Arabidopsis. Plant Cell **19:** 495–508.

**Jackson, D.** (1991). In situ hybridization in plants. In Molecular Plant Pathology: A Practical Approach, D.J. Bowles, S.J. Gurr, and M. McPherson, eds (Oxford, UK: Oxford University Press), pp. 163–174.

**Juarez, M.T., Kui, J.S., Thomas, J., Heller, B.A., and Timmermans, M.C.P.** (2004b). microRNA-mediated repression of *rolled leaf1* specifies maize leaf polarity. Nature **428:** 84–88.

**Juarez, M.T., Twigg, R.W., and Timmermans, M.C.P.** (2004a). Specification of adaxial cell fate during maize leaf development. Development **131:** 4533–4544.

**Kaplan, D.R.** (1975). Comparative developmental evaluation of the morphology of unifacial leaves in the monocotyledons. Bot. Jahrb. **95:** 1–105.

**Kerstetter, R.A., Bollman, K., Taylor, R.A., Bomblies, K., and Poethig, R.S.** (2001). *KANADI* regulates organ polarity in Arabidopsis. Nature **411:** 706–709.

**Kidner, C.A., and Martienssen, R.A.** (2004). Spatially restricted microRNA directs leaf polarity through ARGONAUTE1. Nature **428:** 81–84.

**Kidner, C.A., and Timmermans, M.C.P.** (2007). Mixing and matching pathways in leaf polarity. Curr. Opin. Plant Biol. **10:** 13–20.

**Kim, Y.S., Kim, S.G., Lee, M., Lee, I., Park, H.Y., Seo, P.J., Jung, J.H., Kwon, E.J., Suh, S.W., Paek, K.H., and Park, C.M.** (2008). HD-ZIP III activity is modulated by competitive inhibitors via a feedback loop in Arabidopsis shoot apical meristem development. Plant Cell **20:** 920–933.

**Kumar, S., Tamura, K., and Nei, M.** (2004). MEGA3: Integrated software for Molecular Evolutionary Genetics Analysis and sequence alignment. Brief. Bioinform. **5:** 150–163.

**McConnell, J.R., Emery, J., Eshed, Y., Bao, N., Bowman, J., and Barton, M.K.** (2001). Role of *PHABULOSA* and *PHAVOLUTA* in determining radial patterning in shoots. Nature **411:** 709–713.

**Michelmore, R.W., Paran, I., and Kesseli, R.V.** (1991). Identification of markers linked to disease-resistance genes by bulked segregant analysis - A rapid method to detect markers in specific genomic regions by using segregating populations. Proc. Natl. Acad. Sci. USA **88:** 9828–9832.

**Nelson, J.M., Lane, B., and Freeling, M.** (2002). Expression of a mutant maize gene in the ventral leaf epidermis is sufficient to signal a switch of the leaf's dorsoventral axis. Development **129:** 4581–4589.

**Nelson, T., and Langdale, J.A.** (1992). Developmental genetics of C-4 photosynthesis. Annu. Rev. Plant Physiol. Plant Mol. Biol. **43:** 25–47.

**Nogueira, F.T.S., Madi, S., Chitwood, D.H., Juarez, M.T., and Timmermans, M.C.P.** (2007). Two small regulatory RNAs establish opposing fates of a developmental axis. Genes Dev. **21:** 750–755.

**Ochando, I., Jover-Gil, S., Ripoll, J.J., Candela, H., Vera, A., Ponce, M.R., Martinez-Laborda, A., and Micol, J.L.** (2006). Mutations in the microRNA complementarity site of the *INCURVATA4* gene perturb meristem function and adaxialize lateral organs in arabidopsis. Plant Physiol. **141:** 607–619.

**Otsuga, D., DeGuzman, B., Prigge, M.J., Drews, G.N., and Clark, S. E.** (2001). *REVOLUTA* regulates meristem initiation at lateral positions. Plant J. **25:** 223–236.

**Parkinson, S.E., Gross, S.M., and Hollick, J.B.** (2007). Maize sex determination and abaxial leaf fates are canalized by a factor that maintains repressed epigenetic states. Dev. Biol. **308:** 462–473.

**Prigge, M.J., Otsuga, D., Alonso, J.M., Ecker, J.R., Drews, G.N., and Clark, S.E.** (2005). Class III homeodomain-leucine zipper gene family members have overlapping, antagonistic, and distinct roles in Arabidopsis development. Plant Cell **17:** 61–76.

**Riechmann, J.L., et al.** (2000). Arabidopsis transcription factors: Genome-wide comparative analysis among eukaryotes. Science **290:** 2105–2110.

**Russell, S.H., and Evert, R.F.** (1985). Leaf vasculature in *Zea mays* L. Planta **164:** 448–458.

**Scanlon, M.J.** (2000). NARROW SHEATH1 functions from two meristematic foci during founder-cell recruitment in maize leaf development. Development **127:** 4573–4584.

**Scanlon, M.J.** (2003). The polar auxin transport inhibitor N-1-naphthylphthalamic acid disrupts leaf initiation, KNOX protein regulation, and formation of leaf margins in maize. Plant Physiol. **133:** 597–605.

**Serrano-Cartagena, J., Candela, H., Robles, P., Ponce, M.R., Perez-Perez, J.M., Piqueras, P., and Micol, J.L.** (2000). Genetic analysis of *incurvata* mutants reveals three independent genetic operations at work in Arabidopsis leaf morphogenesis. Genetics **156:** 1363–1377.

**Sharman, B.C.** (1942). Developmental anatomy of the shoot of *Zea mays* L. Ann. Bot. (Lond.) **6:** 245–282.

**Steeves, T.A., and Sussex, I.M.** (1989). Patterns in Plant Development. (Cambridge, UK: Cambridge University Press).

**Sylvester, A.W., Cande, W.Z., and Freeling, M.** (1990). Division and differentiation during normal and *liguleless-1* maize leaf development. Development **110:** 985–1000.

**Timmermans, M.C.P., Schultes, N.P., Jankovsky, J.P., and Nelson, T.** (1998). *Leafbladeless1* is required for dorsoventrality of lateral organs in maize. Development **125:** 2813–2823.

**Waites, R., and Hudson, A.** (1995). *phantastica* - A gene required for dorsoventrality of leaves in *Antirrhinum majus*. Development **121:** 2143–2154.

**Waites, R., Selvadurai, H.R.N., Oliver, I.R., and Hudson, A.** (1998). The *PHANTASTICA* gene encodes a MYB transcription factor involved in growth and dorsoventrality of lateral organs in Antirrhinum. Cell **93:** 779–789.

**Wenkel, S., Emery, J., Hou, B.H., Evans, M.M., and Barton, M.K.** (2007). A feedback regulatory module formed by LITTLE ZIPPER and HD-ZIPIII genes. Plant Cell **19:** 3379–3390.

**Williams, L., Grigg, S.P., Xie, M., Christensen, S., and Fletcher, J.C.** (2005). Regulation of Arabidopsis shoot apical meristem and lateral organ formation by microRNA miR166g and its AtHD-ZIP target genes. Development **132:** 3657–3668.

**Zhong, R., and Ye, Z.H.** (1999). *IFL1*, a gene regulating interfascicular fiber differentiation in Arabidopsis, encodes a homeodomain-leucine zipper protein. Plant Cell **11:** 2139–2152.

**Zhong, R.Q., Taylor, J.J., and Ye, Z.H.** (1999). Transformation of the collateral vascular bundles into amphivasal vascular bundles in an Arabidopsis mutant. Plant Physiol. **120:** 53–64.

**Zhong, R.Q., and Ye, Z.H.** (2004). *amphivasal vascular bundle 1*, a gain-of-function mutation of the *IFL1/REV* gene, is associated with alterations in the polarity of leaves, stems and carpels. Plant Cell Physiol. **45:** 369–385.